CoO Nanoparticles Combined with MRI: Analysis of No-Reflow in Patients with Acute ST-Segment Elevation Myocardial Infarction after PCI and the Effect of Coronary Nicorandil

Xiangwen Liang, Ping Li, Wenchao Xie, Zhihai Lin, Yiyi Li, Wang Liao, Ming Liu*

Department of Cardiology, Yulin First People's Hospital, Yulin 537000, Guangxi Zhuang Autonomous Region, China

ARTICLE INFO	ABSTRACT
	Magnetic resonance imaging (MRI) has become one of the most important medical imaging techniques in the clinic due to its high degree of soft tissue resolution and no radiation damage, and it plays an important role in the early diagnosis and treatment of tumors. This article mainly studies the analysis of no-reflow in patients with acute ST-segment elevation myocardial infarction after PCI and the effect of coronary nicorandil on CoO nanoparticles combined with MRI. In this paper, the synthesized water-soluble nanoparticles are dispersed in a 2% xanthan gum or agarose solution. In an MRI analyzer, the T1 value is tested with the inversion recovery sequence, and the T2 value is tested with the hard pulse CPMG sequence. The gyroscope imaging sequence performs T1-weighted and T2-weighted imaging tests. Calculated densitometry (QCA) was used to measure the stenosis of the coronary lesions, the length of the lesions and the diameter of the lumen before stent implantation. In order to facilitate the collection of urine samples, this article adopts the method of inserting a catheter to drain the patient for sampling. From the baseline state at the time of enrollment to 150 minutes after PCI, polyethylene containing 0.1% butylated hydroxyanisole is used. Urine samples were taken from the test tube every 30 minutes, a total of 6 times were collected, and the collected urine samples were stored in a low-temperature refrigerator at -80℃ for the final inspection. This paper uses calculation software to calculate the risk of death and death/myocardial infarction in the hospital and at 6 months after discharge. The data showed that the postoperatively detected CKMB and cTnI were higher than those before the operation, but the peak value of the nicorandil group was lower than that of the control group, but there was still no statistical difference (P>0.05). The results show that nicorandil can significantly improve the no-reflow phenomenon in AMI patients during PCI.

Introduction

As an important part of coronary heart disease, acute myocardial infarction has also become an important part of the all-cause mortality of human beings. Although the maturity and improvement of percutaneous coronary intervention technology have significantly improved the short-term and long-term prognosis and survival rate of acute myocardial infarction, and PCI is recognized as the safest and most effective treatment of reperfusion. However, no-reflow occurs frequently after PCI, which has a significant impact on the clinical diagnosis, treatment and prognosis of the whole disease. Therefore, looking for safe and effective drugs that can not only improve the myocardial perfusion level of patients with acute myocardial infarction after PCI, protect myocardial function, but also reduce or prevent the

deterioration of hemodynamics is a problem that has been continuously explored in clinical work (1-3).

The occurrence of no-reflow has multiple influencing factors, accompanied by a variety of pathological changes. With the deepening of the understanding of the mechanism of no-reflow, it is considered to include the following aspects: ischemic injury, reperfusion injury, microvascular dysfunction, distal microthrombotic embolism and individual susceptibility. Of course, the occurrence of no-reflow is usually not caused by one factor. No-reflow will seriously affect the myocardial microcirculation perfusion, so reducing the occurrence of no-reflow can further improve the clinical prognosis of patients with myocardial infarction on the basis of successful PCI operation (1-4).

Emergency PCI after acute myocardial infarction

can open the acutely occluded blood vessels that cause myocardial infarction. Tanveer believes that vascular inflammation and the associated sustained inflammatory response are considered to be the key culprits in the pathogenesis of acute atherosclerotic thrombotic events. ST-segment elevation myocardial infarction is considered to be one of the main clinical forms of ACS. He discussed the correlation between hs-CRP levels and the clinical and angiographic features of STEMI, various other traditional risk factors, complications of myocardial infarction, and CAD with angiographic significance. Although his research has a certain reference effect, it lacks necessary experimental content (1). Schiele believes that nursing quality assessment is an indispensable part of modern medical care and has become an indispensable tool for health authorities, the public, the press and patients. Other professional associations have issued QIs to assess the quality of care for acute myocardial infarction (AMI), but there are no such indicators in Europe. In this case, the European Society of Cardiology (ESC) Acute Cardiovascular Care Association (ACCA) reflected on the AMI's care quality measurement and created a group of QIs with a view to developing plans to improve the care of AMI management throughout Europe quality. Although his theory is correct, it is not comprehensive enough (2). Lang believes that stem cell-based regenerative therapy for the treatment of ischemic myocardium is currently the subject of intensive research. In human phases I and II clinical trials, a variety of cell populations have been proved to be safe and have played some positive effects, but there is still a lack of conclusive evidence of efficacy. Although the relevance of animal models for proper preclinical safety and efficacy testing in phase III studies continues to increase, concerns have arisen about the effectiveness of mouse models in predicting clinical outcomes. Against the background of hundreds of pre-clinical studies that have evaluated the efficacy of various cell preparations (including pluripotent stem cells) on heart repair, he systematically re-evaluated the data of the mouse model, which is the first mouse model that paved the way. Although his research has a certain value, it lacks innovation (3). Carlsson believes that high-sensitivity cardiac troponin T (hs-cTnT) has recently been introduced into clinical practice. He included 11,847 chest pain patients and at least one hs-cTnT measurement between 2011 and 2012. He excluded patients with elevated hs-cTnT levels due to any acute cause. He used logistic regression analysis to calculate the adjusted odds ratio with a 95% confidence interval for the association between patient characteristics and hs-cTnT levels> 14ng/L. He also determined the 50th, 75th, 97.5 and 99% percentages of hs-cTnT levels related to age, gender, estimated glomerular filtration rate (eGFR), and the presence of comorbidities. Although his research is more accurate, it lacks clear experimental results (4).

In this paper, through the high-temperature liquid-phase reduction method and the liquid phase decomposition method, the Co/CoO core/shell structure nanoparticle system with a controllable shell thickness was successfully obtained. This study included the long-term medication factors of patients before the onset of the study, aiming to explore the clinical characteristics, risk factors and impact of the no-reflow phenomenon in interventional recanalization of myocardial infarction and further improve the level of clinical diagnosis and treatment. This study aims to explore whether intravenous nicorandil has a protective effect on renal function and possible mechanisms in patients with acute coronary syndrome combined with diabetes after PCI, and to provide more ideas and methods for clinical prevention of CIN.

Acute ST-Segment Elevation Myocardial Infarction
CoO Nanoparticles

The unique properties of nanomaterials, especially the small size effect of nanomaterials, give magnetic nanomaterials excellent magnetic properties. The morphology and structure of cobalt nanoparticles are shown in Figure 1. With the increase of the thickness of the antiferromagnetic shell, the exchange bias of the system increases non-monotonously. When the shell thickness and core size are the same, the exchange bias is at its maximum. The changing trend of coercivity is similar to exchange bias. And the blocking temperature of the sample system does not change with the core size and shell thickness (5).

The phase change of the magnetic moment caused by the magnetic field generated by the small magnetic nanoparticles accelerates the spin-spin relaxation. In

this process, the main relaxation mechanism is the peripheral dipole interaction between the spin of water protons and the magnetic moment of the nanoparticles (6). The expression of spin-spin relaxation is as follows:

$$R_2 = \frac{1}{T_2} = \frac{a}{d_{NP}D}\gamma^2\mu^2 C_{NP}J(\omega,\tau_D) \qquad [1]$$

Where a is a constant, d_{NP} is the diameter of the nanoparticle, and D is the diffusion coefficient.

In the input continuous image sequence, the gray value change of each independent pixel is subject to a single Gaussian probability function, then the Gaussian model of the nanoparticle is:

$$\mu_0(x,y) = \frac{1}{T}\sum_{i=0}^{T-1} f_i(x,y) \qquad [2]$$

$$\sigma_0^2(x,y) = \frac{1}{T}\sum_{i=0}^{T-1}[f_i(x,y)-\mu_0(x,y)]^2 \qquad [3]$$

In the formula, $f_i(x,y)$ represents the gray value of the i-th particle in the image.

Nanomaterials have attracted more and more attention in the field of drug release. By encapsulating drugs in nanocarriers, and modifying them to give the carrier targeting and stimulus responsiveness, the targeted release of drugs in tumor tissues can be achieved. The ideal drug carrier should have the characteristics of stable structure, high drug loading rate, good biocompatibility, low drug leakage and early release, and stimulus-responsive drug release (7-8). Its expression is as follows:

$$D = \frac{RT}{N_0}\bullet\frac{1}{3\pi\eta d} = \frac{k_B}{3\pi\eta d} \qquad [4]$$

In the formula, η is the viscosity of the solvent (dispersion medium), and T is the temperature of the dispersion system. In the case of chains composed of spherical particles, the coercive force is:

$$H_{cn} = \mu(6K_n - 4L_n)/d^3 \qquad [5]$$

$$K_n = \sum_{j=1}^{n}(n-j)/nj^3 \qquad [6]$$

$$L_n = \sum_{j=1}^{\frac{1}{2}(n-1)<j\le\frac{1}{2}(n+1)}[n-(2j-1)]/[n(2j-1)^3] \qquad [7]$$

In the formula, n is the number of particles in the ball chain, μ is the particle magnetic moment, and d is the particle spacing.

The techniques for synthesizing amphiphilic copolymers usually include methods such as ring-opening polymerization, ATRP polymerization, and RAFT polymerization. The calculation formula is as follows.

$$E(r) = E_g(r=\infty) + h^2\pi^2/2\mu r^2 - 1.786e^2/\varepsilon r - 0.248E_{Ry} \qquad [8]$$

In the formula, $E(r)$ is the absorption band gap of the nanoparticle, and $E_g(r=\infty)$ is the band gap of the bulk phase.

The relationship between scattered light intensity and particle size:

$$I_\theta = \frac{9\pi^2 cv^2}{2\lambda^4 R^2}I_0\cdot\left(\frac{n_2^2-n_1^2}{n_2^2+2n_1^2}\right)(1+\cos^2\theta) \qquad [9]$$

In the formula, I_θ is the intensity of scattered light in the θ direction, and R is the distance from the detector to the sample.

The calculation formula of CMC value is as follows.

$$E(A) = \frac{1}{n}\sum_{i=1}^{n}\frac{\min\{\mu\overline{A}(x_i),v\overline{A}(x_i)\}+\min\{\mu\overset{+}{A}(x_i),v\overset{+}{A}(x_i)\}+\pi\overline{A}(x_i)+\pi\overset{+}{A}(x_i)}{\max\{\mu\overline{A}(x_i),v\overline{A}(x_i)\}+\max\{\mu\overset{+}{A}(x_i),v\overset{+}{A}(x_i)\}+\pi\overline{A}(x_i)+\pi\overset{+}{A}(x_i)} \qquad [10]$$

$$f(x_1,y_1,x_2,y_2) = \frac{e^{1-z_1}(1-x_1)+e^{y_1}y_1}{e^{1-z_1}+e^{y_1}}+\frac{e^{1-z_2}(1-x_2)+e^{y_2}y_2}{e^{1-z_2}+e^{y_2}} \qquad [11]$$

The distribution function of electron density is:

$$\rho[r] = \sum_\sigma\rho_\sigma\sum_{i=1}^{N_\sigma}\rho_{i\sigma}(r) = \sum_\sigma\sum_{i=1}^{N_\sigma}|\varphi_{i\sigma}(r)|^2 \qquad [12]$$

In the formula, $\varphi_{i\sigma}(r)$ is the energy level of the electron. When dealing with spin polarization by the local density approximation method, the exchange energy form can be written as:

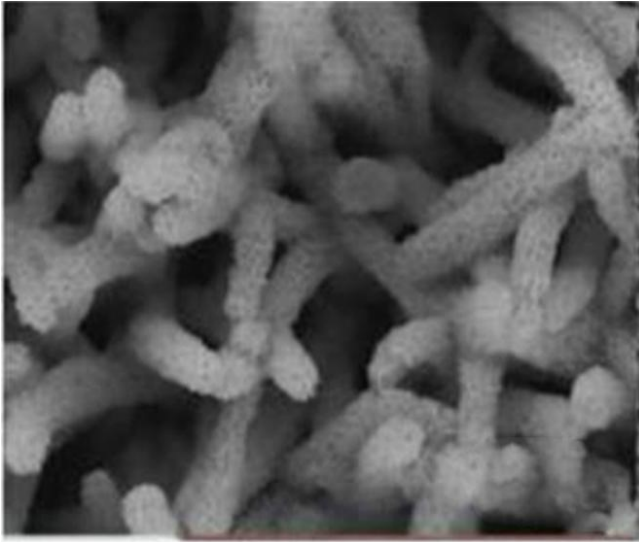$$E_x[\rho_\alpha,\rho_\beta] = \frac{1}{2}E_x^0[2\rho_\alpha]+\frac{1}{2}E_x^0[2\rho_\beta] \qquad [13]$$

Figure 1. The morphology and structure of cobalt nanoparticles (picture from http://alturl.com/ho498)

MRI

The countless hydrogen nuclei in the human body move in disorder, and they are arranged in no direction so that their magnetic fields cancel each other out. The entire human body is not magnetic. However, when in a uniform magnetic field, the spin axis of the small magnet hydrogen nucleus will follow the direction of the magnetic field. Re-arranged in an orderly manner, and in a fast conical rotation, in this state, with a specific frequency of radio frequency pulse excitation, the hydrogen nucleus will absorb a certain amount of energy and resonate, that is, nuclear magnetic resonance. Nowadays, calcium ion antagonists are clinically used to prevent and treat no-reflow, mainly to inhibit the effect of vasoconstrictors (9-10).

Acute ST-Segment Elevation Myocardial Infarction

STEMI is a group of clinical syndrome with myocardial ischemia symptoms and ECG suggesting ST-segment elevation and myocardial necrosis markers. Arrhythmia, shock or heart failure, and even sudden death may occur, which requires timely treatment to reduce mortality. In the case of no residual stenosis after stent implantation, the evaluation of coronary blood flow is particularly important. The purpose of reperfusion is to restore normal blood flow to the heart tissue, not just to open the epicardial artery (11). Therefore, slow coronary flow or no-reflow phenomenon is a sign of poor prognosis of patients after coronary artery opening.

Blood flow can not enter or leave the necrotic myocardium, resulting in poor healing of infarcted myocardium and left ventricular remodeling, which is an important reason to increase the risk of major adverse cardiac events, including heart rupture, congestive heart failure and death (12).

The mechanism of no-reflow in emergency PCI has not yet been established. It may be related to the impairment of the endothelial function of the coronary artery, atherosclerotic material shedding and embolizing distal small vessels, local myocarditis, endothelial cell edema, microcirculation spasm, platelet activation, degranulation, the release of inflammatory mediators and vasoconstrictors. For the prevention and treatment of no-reflow, it includes instrument treatment and drug treatment (13). However, with the accumulation of surgical experience, cardiovascular interventional physicians have found that some patients will have a no-reflow phenomenon after PCI treatment. Coronary angiography shows that although the large coronary artery has been opened and the forward blood flow is restored, there is no blood flow or slow blood flow and delayed emptying in the distal microvessel of the ischemic area, and the myocardial tissue can not be effectively reperfused, At the same time, coronary dissection, intimal tear, spasm and thromboembolism were excluded (14).

The appearance of no-reflow reduces the clinical benefit of patients receiving coronary intervention therapy, brings adverse prognosis to patients, and even leads to death. ATP sensitive K + channel opening. KATP channel links the electrical activity on the membrane surface with the metabolic activity of cells. Channel opening can reduce the intracellular calcium concentration, especially the T-type calcium channel on the microvessel. The decrease of calcium concentration is manifested by dilating the coronary artery and increasing the coronary blood flow, especially significantly dilating the microvessel and improving the blood oxygen of the ischemic myocardium (15). The delay of reperfusion time can not only significantly increase the incidence of no-reflow but also increase the thrombus load in the coronary artery, further aggravate the degree of ischemia, and significantly reduce the rate of normal blood flow (16).

The patients with different thrombus loads were divided into different groups. The results showed that if the blood flow of AMI patients with severe thrombus load was restored within 6 hours, the occurrence of no-reflow after PCI could be significantly reduced. Nicorandil can improve myocardial ischemia by relaxing the smooth muscle of the coronary artery, dilating the blood vessel and increasing the blood flow of the coronary artery. Nicorandil has a variety of beneficial effects on the cardiovascular system. In addition to improving the postconditioning of myocardial ischemia and myocardial protection, nicorandil can also resist thrombosis, improve fibrinolysis and promote angiogenesis. In addition, nicorandil can also improve coronary microcirculation, thereby improving the cardiac function and clinical prognosis of patients with coronary heart disease (17-18).

Materials and methods
No-reflow Experiment after PCI in Patients with Acute ST-Segment Elevation Myocardial Infarction
Subject
Patients who received reperfusion therapy or thrombolytic therapy were definitely diagnosed as acute myocardial infarction, regardless of race, gender, or nationality. The diagnosis of AMI meets the WHO diagnostic criteria: typical chest pain lasts> 30 minutes, ECG shows obvious ST-segment changes within 12 hours before infarction, ST-segment elevation or depression in two or more consecutive leads> 0.1mV, Myocardial blood markers such as acid kinase increase more than three times the normal value (19-20).

MRI Experiment
Disperse the synthesized water-soluble nanoparticles in a 2% xanthan gum or agarose solution. In an MRI analyzer, use the inversion recovery sequence to test the T1 value, use the hard pulse CPMG sequence to test the T2 value, and use the spin back. The wave imaging sequence performs T1-weighted and T2-weighted imaging tests. Computer densitometry (QCA) was used to measure the degree of stenosis, the length of the lesion and the diameter of the lumen of the coronary artery lesion before stent implantation (21).

Emergency PCI and Urine Sample Collection
PCI operation is performed by the same surgeon and uses the same brand of the guide wire, balloon and drug-eluting stent. During the operation, heparinized anticoagulation is performed according to body weight, and nitroglycerin (0.1 mg/time) is injected into the coronary artery. Continue intravenous anticoagulation with heparin for 48 hours to keep APTT at 1.5-2 times the baseline value. All patients' PCI operations were performed within 60 minutes after the patient was admitted to the hospital, and the final patient's coronary angiography showed that the residual stenosis must be less than 25% (Lumen diameter). In order to facilitate the collection of urine samples, this article adopts the method of inserting a catheter to drain the patient for sampling. From the baseline state at the time of enrollment to 150 minutes after PCI, polyethylene containing 0.1% butylated hydroxyanisole is used. Urine samples were taken from the test tube every 30 minutes, a total of 6 times were collected, and the collected urine samples were stored in a low-temperature refrigerator at -80°C for final inspection (22-23).

Reperfusion Arrhythmia
This experimental study recorded and compared the occurrence of reperfusion arrhythmia within 5 minutes after coronary intervention in patients in the nicorandil group and simple PCI group, which can be used to evaluate the severity of ischemia/reperfusion injury in acute myocardial infarction to a certain extent (24). Venous blood samples were collected from all patients in the nicorandil group and simple PCI group immediately after admission, 0, 12 and 24 hours after PCI, respectively, to monitor the changes in cardiac troponin I (cTnI) level in acute myocardial injury so as to determine the degree of myocardial injury after primary PCI in acute ST-segment elevation myocardial infarction (25).

GRACE Risk Score
The calculation software separately calculates the risk of death and death/myocardial infarction in the hospital and at 6 months after discharge. This article mainly involves the analysis of the adverse prognosis during hospitalization. Therefore, the former part of the software is used. Specifically, 8 indicators (values) at admission: age, heart rate, Blood pressure, serum

creatinine level, Killip grade of heart failure, cardiac arrest before admission, ST-segment downshift, and elevated myocardial enzyme levels (26). The specific score results are obtained after software calculation, and the preliminary evaluation method is shown in Table 1.

Table 1. Evaluation method

Danger level	GRACE score	Risk of death in hospital (%)
Low risk	≤108	<1
In danger	109-140	1-3
High risk	>140	>3

Statistical Analysis

Use SPSS20.0 statistical program for statistical analysis. If the variances of the two groups of measurement data are homogeneous, the independent-sample t-test is used for analysis, if the variances are not uniform, the Wilcoxon rank-sum test is used; the count data is expressed as a percentage, and the comparison is analyzed by the chi-square test; $P<0.05$ is There are statistical differences (27-28).

Results and discussion
Multi-Factor Analysis of No-Reflow Related Risks
Comparison of biochemical indicators of different groups

The TEM image of CoO nanoparticles is shown in Figure 2. It can be clearly seen from the figure that the experimentally synthesized CoO nanoparticles are nanorod-shaped, with an average rod length of 28nm and an average rod width of 9.5nm. Nanoparticles are composed of longer rod-shaped particles and smaller short rod-shaped nanoparticles. The 111 crystal plane of the cubic phase can be found from the high-resolution transmission electron microscope. At the same time, the selected area electron diffraction is significantly different from the single cubic phase nanoparticles obtained by the reaction for 2h. It further shows that different reaction times have an effect on the crystal phase of CoO nanoparticles, which may be related to the crystal plane growth of nanoparticles in different times.
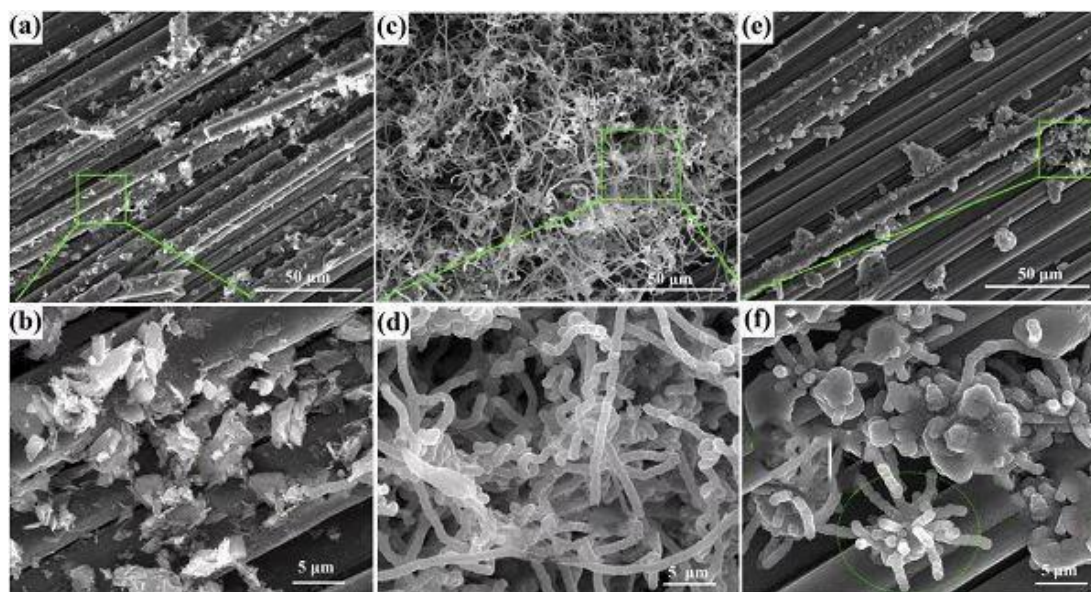

Figure 2. TEM image of CoO nanoparticles (picture from http://alturl.com/m9p67)

Table 2 shows the average grain size and room temperature magnetic performance parameters of cobalt nanoparticles synthesized under different feeding methods. The crystal structure of cobalt nanoparticles synthesized by the high-temperature injection method and the low-temperature heating method is the same, and the average crystal grain size does not change much. The average grain size of the cobalt nanoparticles does not change with the reaction

temperature but shows a linear relationship. As the reaction temperature decreases, the average grain size first increases and then decreases. This may be because when the temperature is lowered from 260°C to 240°C, the growth rate of the particles is greater than the nucleation rate of the crystal, so the particle size increases. When the temperature continues to decrease to 220℃, the growth rate of crystal grains is lower than the nucleation rate, resulting in a decrease

in particle size. However, when the reaction temperature is as low as 200°C, the reaction temperature is too low and crystals cannot be formed. Therefore, when synthesizing cobalt nanoparticles, the reaction temperature in the experiment must be higher than 200°C.

Table 2. Average grain size and room temperature magnetic performance parameters of cobalt nanoparticles synthesized under different feeding methods

Feeding method	Crystal structure	Grain size (nm)	Ms(emu/g)	Mr(emu/g)	Hc(Oe)
High temperature injection	hcp	5.9±0.4	130.3	26.2	283.1
Low temperature heating method	hcp	6.4±0.3	98.9	24.7	469.2

The number distribution of patients with different risk levels in the model group and validation group of the basic population is shown in Table 3 and Figure 3. In the model group, patients with no-reflow phenomenon scored 12.4%, 67.6% and 20.0% in low-risk, medium risk and high-risk areas, respectively. Most patients were in the medium risk area. Patients without the no-reflow phenomenon scored 23.1%, 72.0% and 4.9% in low-risk, medium risk and high-risk areas, respectively, and less than 1 / 20 in high-risk areas. Record the reperfusion arrhythmia of patients in the nicorandil group and the control group after the opening of infarct-related vessels. It was found that the occurrence of rapid and slow arrhythmia in the nicorandil group was less than that in the control group, with a statistical difference (P < 0.05).

Table 3. The distribution of the number of patients with different risk levels in the basic population model group and verification group

Score	Model group				Verification group			
	No-reflow (n=306)		Normal blood flow (n=732)		No-reflow (n=149)		Normal blood flow (n=346)	
	Number	Rate	Number	Rate	Number	Rate	Number	Rate
Low risk	38	12.4%	169	23.1%	14	9.4%	91	26.3%
In danger	207	67.6%	527	72.0%	113	75.8%	219	63.3%
High risk	61	20.0%	36	4.9%	22	14.8%	36	10.4%

The particle size tracking of CoO nanoparticles in different solutions is shown in Figure 4. The magnetization value increases with the increase of the applied magnetic field, but the relationship between the two is not linear. Only when the amount of alkali added makes the pH of the reaction system greater than 10, the reaction can proceed smoothly, but when the pH of the reaction system is greater than 12, the

ionic strength is too high, which is not conducive to the encapsulation of dextran. Within a certain range, the larger the amount of alkali, the smaller the particle size.
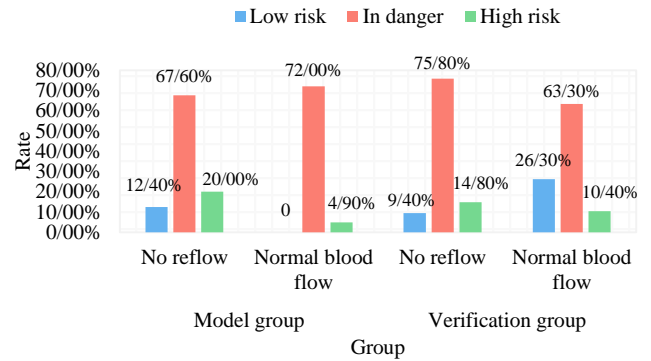

Figure 3. The distribution of the number of patients with different risk levels in the basic population model group and verification group
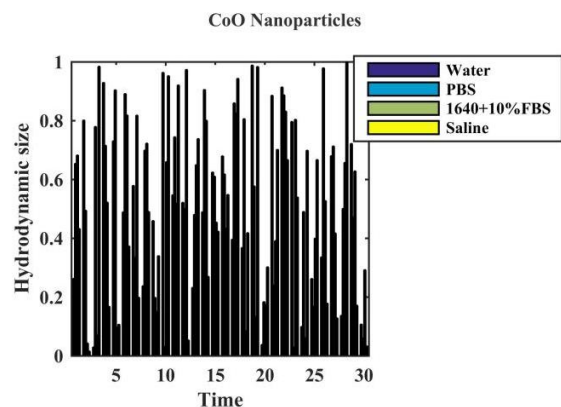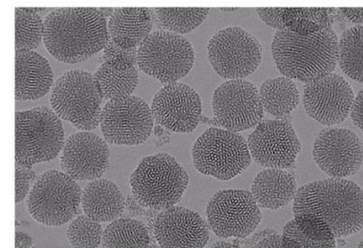

Figure 4. Particle size tracking of CoO nanoparticles (up) and their hydrodynamic size in different times and solutions (down)

Multi-Factor Analysis of Emergency Coronary Angiography without Reflow

A comparison of related parameters of myocardial injury markers is shown in Table 4. The preoperative creatine kinase isoenzyme CK-MB and troponin I were not significantly different between the two groups of patients (P>0.05). The postoperatively detected CKMB and cTnI were higher than those

before the operation, but the peak value of the nicorandil group was lower than that of the control group, but there was still no statistical difference (P>0.05).

Table 4. Comparison of related parameters of myocardial injury markers

Project		Nicorandil group	Control group	P value
CK-MB (ng/ml)	Preoperative	81.8±24.7	83.6±25.9	0.867
	Postoperative peak	89.6±36.8	90.7±35.2	0.442
cTnI (ng/ml)	Preoperative	11.09±1.68	10.74±0.96	0.347
	Postoperative peak	12.96±2.23	12.14±2.44	0.767

The toxicity of ngca to normal cells before and after oxidation is shown in Figure 5. The toxicity of ngca-2 to BEAS-2B cells before oxidation was greater than that of ongca-2 after oxidation. When the concentration of ngca-2 was 5 μ g / ml before oxidation, the survival rate of BEAS-2B cells was less than 50%. When the concentration of ngca-2 was 5 μ g / ml after oxidation, the survival rate of BEAS-2B cells was about 80%. When the concentration of ongca-2 was 500 μ g / ml after oxidation, the survival rate of BEAS-2B cells was about 50%; when ngca-2 concentration was 500 μ g / ml, the survival rate of BEAS-2B cells was less than 10%.
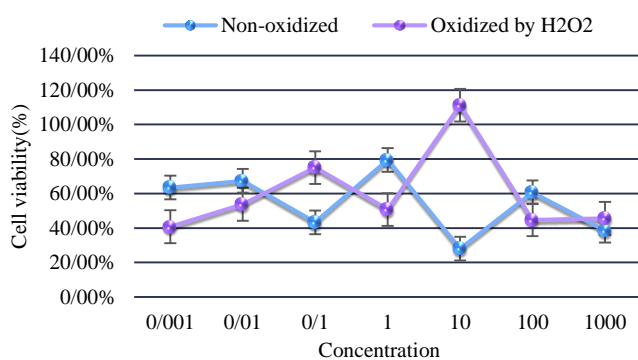

Figure 5. Toxicity of NGCA to normal cells before and after oxidation

The multivariate logistic regression analysis without reflow is shown in Table 5. With no-reflow as the dependent variable, a Logistic regression analysis was performed. The results showed that the time from angina pectoris to the perpetrator's vessel opening, BMI, TC, and LYM/NEUT enter the equation, which are independent risk factors for no-reflow after PCI, and their relative risks are respectively It is 7.627, 0.528, 2.631, 3.402. Therefore, the activity of SOD indirectly reflects the ability to inhibit OFR. The

increase in MDA in cells is mostly due to the destruction of biofilms by oxygen-free radicals. Therefore, through the measurement of MDA, we can indirectly harden the extent of oxygen-free radical damage in the body.

Table 5. Multivariate logistic regression analysis without reflow

Variable	B	OR	95%CI of OR	P
Ischemic time	0.145	1.156	1.051	0.003
Homocysteine	0.278	1.321	1.172	<0.001
TIMI blood flow before intervention	-0.962	0.382	0.148	0.047
High thrombus load	1.182	3.260	1.188	0.022

Table 6 shows the relationship between the ST segment fall rate and the improvement of coronary blood flow. There are 28 patients with an ECG ST-segment fall rate greater than 50%, accounting for 64%, and 16 patients with an ECG ST-segment fall rate less than or equal to 50%, which is 36%. After medication, there were 40 patients with TIMI blood flow greater than grade 2, of which 30% of patients had ST-segment fall rate less than or equal to 50%, and the number of cTFC blood flow frames was less than 27.2 in 38 cases. Among them, 29% of patients had an ST-segment fall. The rate is less than or equal to 50%, and there are 32 cases with TMPG blood flow classification greater than level 2. Among them, 14% of the patients, the ST segment fall rate is less than or equal to 50%.

Table 6. The relationship between ST-segment fall rate and coronary blood flow improvement

	ST-segment fall rate is greater than 50%	ST-segment fall rate is less than or equal to 50%
TIMI classification>2 (n=40)	70%	30%
cTFC frame number<27.2 (n=38)	71%	29%
TMPG classification>2 (n=32)	86%	14%

Comparison of Ischemia-Reperfusion Injury

The morphological characteristics of coronary angiography in the group with and without reflow phenomenon are shown in Figure 6. There was no significant difference in the number of cases of infarction-related arteries with spasm and dissection between the group with the no-reflow phenomenon and the group without no-reflow phenomenon (P>0.05). However, there was a significant difference between the two groups in the number of cases with

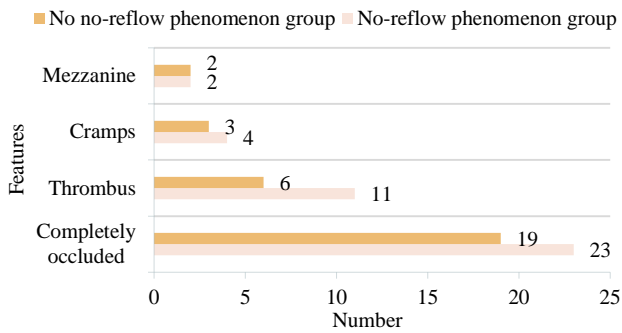complete occlusion of infarction-related arteries and signs of thrombosis (P<0.05).

Figure 6. Angiographic morphological characteristics

Figure 7 shows the comparison of the incidence of PMI between the two groups of patients after PCI. It can be seen from the figure that compared with the NIT group, the incidence of PMI in the NCD group was significantly lower (P=0.03). The incidence of cTnI value exceeding 3 times in the nicorandil group was lower than that in the control group (P=0.029). The incidence of cTnI value exceeding 5 times in the nicorandil group was lower than that in the control group (P=0.036).
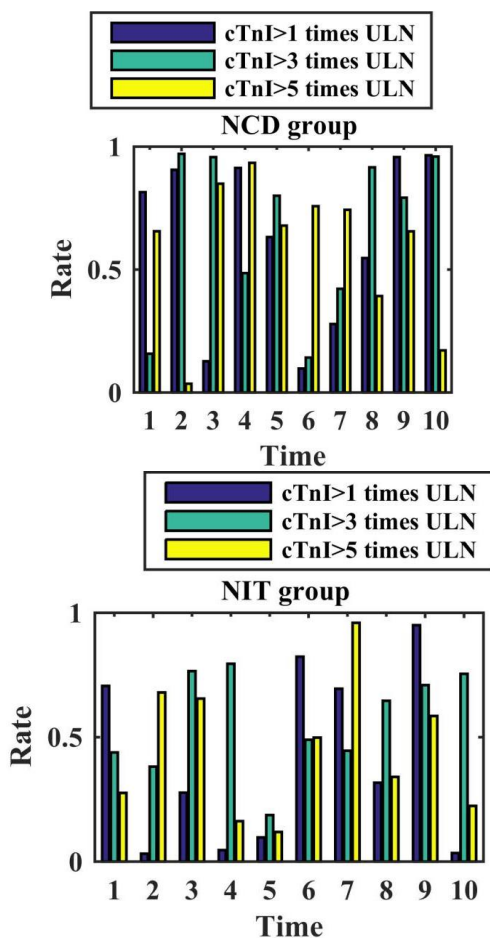

Figure 7. Comparison of the incidence of PMI between the two groups of patients after PCI

Figure 8 shows the comparison of ischemia, infarction, and non-reflow area after myocardial ischemia-reperfusion in each group. After 45 minutes of ischemia and 120 minutes of reperfusion, the levels of myocardial enzymes and isoenzymes in the model group increased significantly, indicating that myocardial cells were acutely injured. Compared with the model group, the levels of myocardial enzymes in the nicorandil group and adenosine group were significantly lower, with a statistically significant difference (P<0.01). And nicorandil had a better effect in reducing serum CK and CK-MB compared with the adenosine group; the difference was statistically significant (P<0.01). There was no significant difference in AAR/TA between the model group, adenosine group and nicorandil group, indicating that the range of coronary vascular ischemia in each group was roughly the same. Compared with the model group, the myocardial infarction area (NA/AAR%) and no-reflow area (ANR/AAR%) of the adenosine group and nicorandil group were significantly reduced (P<0.01). It shows that nicorandil and adenosine can reduce the area of myocardial infarction, improve coronary perfusion after myocardial infarction, and increase the ratio of myocardial reflow after myocardial reperfusion (29-38).
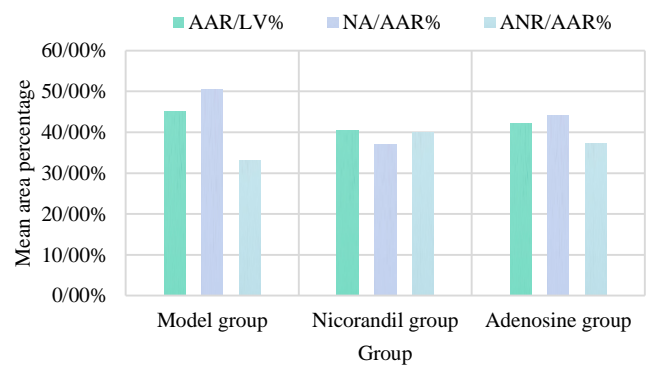

Figure 8. Comparison of ischemia, infarction and non-reflow area after myocardial ischemia reperfusion in each group

Conclusions

Three experienced interventional physicians evaluated TIMI blood flow classification according to CAG images after PCI, evaluated and recorded IRA blood flow and myocardial reperfusion. ECG was reexamined about 1 hour after PCI to observe str;

according to the CAG image evaluation and STR comprehensive evaluation, the serum PCT level, the reported risk factors of NRP and the incidence of NRP events were compared between the two groups. Compared with the control group, the serum PCT level of STEMI patients with no-reflow phenomenon after PCI was higher, but the PCT level could not be used as a predictor of the no-reflow phenomenon.

After intravenous application of nicorandil in patients with acute myocardial infarction after PCI, the wall motion integral index of the treatment group was better; the left ventricular end-systolic volume index of the treatment group was lower; the coronary microcirculation perfusion of the treatment group was better. It can be seen that compared with nitroglycerin, nicorandil can reduce the wall motion integral index, improve the coronary microcirculation function, relieve the symptoms of angina pectoris after myocardial infarction, reduce malignant arrhythmia, and reduce the occurrence of recurrent angina pectoris. The co nanotube / magnetic nanoparticles hybrid material studied in this paper has low cytotoxicity and hemolytic effect; it has high DOX drug loading and little drug release under normal physiological conditions; its MRI imaging effect in vivo is obvious, so it can be used as MRI imaging agent.

Prophylactic intracoronary administration of different doses of nicorandil can improve the myocardial perfusion level of IRA reperfusion area, reduce the occurrence of myocardial injury and no-reflow, inhibit the inflammatory reaction after PCI, and reduce the level of inflammatory transmitter after IRA opening. Nicorandil can inhibit the production of reactive oxygen species (ROS), alleviate the no-reflow phenomenon, improve coronary microcirculation disorder, inhibit cardiac sympathetic nerve activity, resist myocardial cell apoptosis, protect myocardial cell mitochondrial function, so as to reduce left ventricular end-diastolic volume (index) and left ventricular end-systolic volume (index), improve left ventricular ejection fraction, and reduce clinical cardiac events.

Acknowledgments

Interest conflict
The authors declare that they have no conflict of interest.

References
1. Tanveer S, Banu S, Jabir NR, Khan MS, Ashraf GM, Manjunath NC, Tabrez S. Clinical and angiographic correlation of high-sensitivity C-reactive protein with acute ST elevation myocardial infarction. Exp Ther Med. 2016 Dec;12(6):4089-4098. doi: 10.3892/etm.2016.3882. Epub 2016 Nov 8. PMID: 28105138; PMCID: PMC5228442.
2. Schiele F, Gale CP, Bonnefoy E, Capuano F, Claeys MJ, Danchin N, Fox KA, Huber K, Iakobishvili Z, Lettino M, Quinn T, Rubini Gimenez M, Bøtker HE, Swahn E, Timmis A, Tubaro M, Vrints C, Walker D, Zahger D, Zeymer U, Bueno H. Quality indicators for acute myocardial infarction: A position paper of the Acute Cardiovascular Care Association. Eur Heart J Acute Cardiovasc Care. 2017 Feb;6(1):34-59. doi: 10.1177/2048872616643053. Epub 2016 Sep 20. PMID: 27574334.
3. Lang CI, Wolfien M, Langenbach A, Müller P, Wolkenhauer O, Yavari A, Ince H, Steinhoff G, Krause BJ, David R, Glass Ä. Cardiac Cell Therapies for the Treatment of Acute Myocardial Infarction: A Meta-Analysis from Mouse Studies. Cell Physiol Biochem. 2017;42(1):254-268. doi: 10.1159/000477324. Epub 2017 May 25. PMID: 28535507.
4. Carlsson AC, Bandstein N, Roos A, Hammarsten O, Holzmann MJ. High-sensitivity cardiac troponin T levels in the emergency department in patients with chest pain but no myocardial infarction. Int J Cardiol. 2017 Feb 1;228:253-259. doi: 10.1016/j.ijcard.2016.11.087. Epub 2016 Nov 9. PMID: 27865194.
5. Spadaccio C, Nappi F, De Marco F, Sedati P, Taffon C, Nenna A, Crescenzi A, Chello M, Trombetta M, Gambardella I, Rainer A. Implantation of a Poly-L-Lactide GCSF-Functionalized Scaffold in a Model of Chronic Myocardial Infarction. J Cardiovasc Transl Res. 2017 Feb;10(1):47-65. doi: 10.1007/s12265-016-9718-9. Epub 2017 Jan 23. PMID: 28116550; PMCID: PMC5323505.
6. Mohammadi R, Khodakarim S, Alipour A, Bitaraf E, Soori H. Association between Air Temperature and Acute Myocardial Infarction Hospitalizations in Tehran, Iran: A Time-Stratified Case-Crossover. Int J Occup Environ Med. 2017 Jul;8(3):143-152. doi: 10.15171/ijoem.2017.1069. PMID: 28689211; PMCID: PMC6679627.
7. Pasupathy S, Tavella R, Beltrame JF. Myocardial Infarction With Nonobstructive Coronary Arteries (MINOCA): The Past, Present, and Future Management. Circulation. 2017 Apr 18;135(16):1490-1493. doi: 10.1161/CIRCULATIONAHA.117.027666. PMID: 28416521.
8. Hoedemaker NP, Roolvink V, de Winter RJ, van Royen N, Fuster V, García-Ruiz JM, Er F, Gassanov N, Hanada K, Okumura K, Ibáñez B, van 't Hof AW, Damman P. Early intravenous beta-blockers in patients undergoing primary percutaneous coronary intervention for ST-segment elevation myocardial

infarction: A patient-pooled meta-analysis of randomized clinical trials. Eur Heart J Acute Cardiovasc Care. 2020 Aug;9(5):469-477. doi: 10.1177/2048872619830609. Epub 2019 Feb 14. PMID: 30759994; PMCID: PMC7672673.

9. Tarantini G, D'Amico G, Brener SJ, Tellaroli P, Basile M, Schiavo A, Mojoli M, Fraccaro C, Marchese A, Musumeci G, Stone GW. Survival After Varying Revascularization Strategies in Patients With ST-Segment Elevation Myocardial Infarction and Multivessel Coronary Artery Disease: A Pairwise and Network Meta-Analysis. JACC Cardiovasc Interv. 2016 Sep 12;9(17):1765-76. doi: 10.1016/j.jcin.2016.06.012. PMID: 27609250.

10. Bons LR, Dabiri-Abkenari L, VAN Domburg RT, Szili-Torok T, Zijlstra F, Theuns DA. The Effect of Elapsed Time from Myocardial Infarction on Mortality and Major Adverse Cardiac and Cerebrovascular Events in ICD Patients. Pacing Clin Electrophysiol. 2015 Dec;38(12):1448-55. doi: 10.1111/pace.12739. Epub 2015 Oct 1. PMID: 26289034.

11. Carberry J, Carrick D, Haig C, Rauhalammi SM, Ahmed N, Mordi I, McEntegart M, Petrie MC, Eteiba H, Hood S, Watkins S, Lindsay M, Davie A, Mahrous A, Ford I, Sattar N, Welsh P, Radjenovic A, Oldroyd KG, Berry C. Remote Zone Extracellular Volume and Left Ventricular Remodeling in Survivors of ST-Elevation Myocardial Infarction. Hypertension. 2016 Aug;68(2):385-91. doi: 10.1161/HYPERTENSIONAHA.116.07222. Epub 2016 Jun 27. PMID: 27354423; PMCID: PMC4956675.

12. Hung WH, Chang CC, Ho SY, Liao CY, Wang BY. Systemic air embolism causing acute stroke and myocardial infarction after percutaneous transthoracic lung biopsy-a case report. J Cardiothorac Surg. 2015 Sep 15;10:121. doi: 10.1186/s13019-015-0329-3. PMID: 26374639; PMCID: PMC4571114.

13. Beygui F, Cayla G, Roule V, Roubille F, Delarche N, Silvain J, Van Belle E, Belle L, Galinier M, Motreff P, Cornillet L, Collet JP, Furber A, Goldstein P, Ecollan P, Legallois D, Lebon A, Rousseau H, Machecourt J, Zannad F, Vicaut E, Montalescot G; ALBATROSS Investigators. Early Aldosterone Blockade in Acute Myocardial Infarction: The ALBATROSS Randomized Clinical Trial. J Am Coll Cardiol. 2016 Apr 26;67(16):1917-27. doi: 10.1016/j.jacc.2016.02.033. PMID: 27102506.

14. Bohn B, Schöfl C, Zimmer V, Hummel M, Heise N, Siegel E, Karges W, Riedl M, Holl RW; DPV-initiative. Achievement of treatment goals for secondary prevention of myocardial infarction or stroke in 29,325 patients with type 2 diabetes: a German/Austrian DPV-multicenter analysis. Cardiovasc Diabetol. 2016 May 3;15:72. doi: 10.1186/s12933-016-0391-8. PMID: 27141979; PMCID: PMC4855873.

15. Karetnikova NV, Barbarash LO, Katsyuba VM, Polikutina MO, Slepynina SY. [Diffusion Capacity of the Lung and Maladaptive Post-Infarction Remodeling of the Heart]. Kardiologiia. 2017 Aug;57(8):20-27. Russian. doi: 10.18087/cardio.2017.8.10013. PMID: 29041888.

16. Waterford SD, Di Eusanio M, Ehrlich MP, Reece TB, Desai ND, Sundt TM, Myrmel T, Gleason TG, Forteza A, de Vincentiis C, DiScipio AW, Montgomery DG, Eagle KA, Isselbacher EM, Muehle A, Shah A, Chou D, Nienaber CA, Khoynezhad A. Postoperative myocardial infarction in acute type A aortic dissection: A report from the International Registry of Acute Aortic Dissection. J Thorac Cardiovasc Surg. 2017 Mar;153(3):521-527. doi: 10.1016/j.jtcvs.2016.10.064. Epub 2016 Nov 14. PMID: 27932024.

17. Park TE, Yusuff J, Sharma R. Use of aspirin and statins for the primary prevention of myocardial infarction and stroke in patients with human immunodeficiency virus infection. Int J STD AIDS. 2016 May;27(6):447-52. doi: 10.1177/0956462415585448. Epub 2015 May 7. PMID: 25957325.

18. Jasper B, Tobias R, Louise C, Greenslade JH, Parsonage W.A, Christopher H, et al. Two-hour algorithm for triage toward rule-out and rule-in of acute myocardial infarction by use of high-sensitivity cardiac troponin i. Clinic Chem 2016;62(3):369-379.

19. Bonaca MP, Bhatt DL, Storey RF, Steg PG, Cohen M, Kuder J, Goodrich E, Nicolau JC, Parkhomenko A, López-Sendón J, Dellborg M, Dalby A, Špinar J, Aylward P, Corbalán R, Abola MTB, Jensen EC, Held P, Braunwald E, Sabatine MS. Ticagrelor for Prevention of Ischemic Events After Myocardial Infarction in Patients With Peripheral Artery Disease. J Am Coll Cardiol. 2016 Jun 14;67(23):2719-2728. doi: 10.1016/j.jacc.2016.03.524. Epub 2016 Apr 1. PMID: 27046162.

20. Calais F, Lagerqvist B, Leppert J, James SK, Fröbert O. Thrombus aspiration in patients with large anterior myocardial infarction: A Thrombus Aspiration in ST-Elevation myocardial infarction in Scandinavia trial substudy. Am Heart J. 2016 Feb;172:129-34. doi: 10.1016/j.ahj.2015.11.012. Epub 2015 Nov 22. PMID: 26856224.

21. Doig D, Turner EL, Dobson J, Featherstone RL, Lo RT, Gaines PA, Macdonald S, Bonati LH, Clifton A, Brown MM; ICSS Investigators. Predictors of Stroke, Myocardial Infarction or Death within 30 Days of Carotid Artery Stenting: Results from the International Carotid Stenting Study. Eur J Vasc Endovasc Surg. 2016 Mar;51(3):327-34. doi: 10.1016/j.ejvs.2015.08.013. Epub 2015 Oct 24. PMID: 26602322; PMCID: PMC4786052.

22. Weichenthal S, Lavigne E, Evans G, Pollitt K, Burnett RT. Ambient PM2.5 and risk of emergency room visits for myocardial infarction: impact of regional PM2.5 oxidative potential: a case-crossover study. Environ Health. 2016 Mar 24;15:46. doi: 10.1186/s12940-016-0129-9. PMID: 27012244; PMCID: PMC4806515.

23. Anderson JL, May HT, Lappé DL, Bair T, Le V, Carlquist JF, Muhlestein JB. Impact of Testosterone

Replacement Therapy on Myocardial Infarction, Stroke, and Death in Men With Low Testosterone Concentrations in an Integrated Health Care System. Am J Cardiol. 2016 Mar 1;117(5):794-9. doi: 10.1016/j.amjcard.2015.11.063. Epub 2015 Dec 13. PMID: 26772440.

24. Zettler ME, Peterson ED, McCoy LA, Effron MB, Anstrom KJ, Henry TD, Baker BA, Messenger JC, Cohen DJ, Wang TY; TRANSLATE-ACS Investigators. Switching of adenosine diphosphate receptor inhibitor after hospital discharge among myocardial infarction patients: Insights from the Treatment with Adenosine Diphosphate Receptor Inhibitors: Longitudinal Assessment of Treatment Patterns and Events after Acute Coronary Syndrome (TRANSLATE-ACS) observational study. Am Heart J. 2017 Jan;183:62-68. doi: 10.1016/j.ahj.2016.10.006. Epub 2016 Oct 15. PMID: 27979043.

25. Crampton AS, Rötzer MD, Ridge CJ, Yoon B, Schweinberger FF, Landman U, Heiz U. Assessing the concept of structure sensitivity or insensitivity for sub-nanometer catalyst materials. Surface Sci 2016 Oct 1;652:7-19.

26. Yin C, Negreiros FR, Barcaro G, Beniya A, Sementa L, Tyo EC, Bartling S, Meiwes-Broer KH, Seifert S, Hirata H, Isomura N. Alumina-supported sub-nanometer Pt 10 clusters: amorphization and role of the support material in a highly active CO oxidation catalyst. J Materials Chem A. 2017;5(10):4923-31.

27. Yi W, Xiaolan S, Hao H. An elementary fractal thermal conduction theory model for nanometer energetic materials. Chin J Explos Propellants 2018;41:554-61.

28. Norizan MN, Miyazaki Y, Ohishi Y, Muta H, Kurosaki K, Yamanaka S. The nanometer-sized eutectic structure of Si/CrSi2 thermoelectric materials fabricated by rapid solidification. J Electron Mater 2018 Apr;47(4):2330-6.

29. Moradi S, Khaledian S, Abdoli M, Shahlaei M, Kahrizi D. Nano-biosensors in cellular and molecular biology. Cell Mol Biol 2018;64(5):85-90. doi:10.14715/cmb/2018.64.5.14.

30. Alavi, M., Rai, M., Martinez, F., Kahrizi, D., Khan, H., Rose Alencar de Menezes, I., Douglas Melo Coutinho, H., Costa, J. The efficiency of metal, metal oxide, and metalloid nanoparticles against cancer cells and bacterial pathogens: different mechanisms of action. Cell Mol Biomed Reports, 2022; 2(1): 10-21. doi: 10.55705/cmbr.2022.147090.1023.

31. Khaledian S, Abdoli M, Shahlaei M, Behbood L, Kahrizi D, Arkan E, Moradi S. Two-dimensional nanostructure colloids in novel nano drug delivery systems. Colloids Surf A Physicochem Eng Asp 2020 Jan 20;585:124077. doi: 10.1016/j.colsurfa.2019.124077.

32. Darvishi E, Kahrizi D, Arkan E, Hosseinabadi S, Nematpour N. Preparation of bio-nano bandage from quince seed mucilage/ZnO nanoparticles and its application for the treatment of burn. J Mol Liq 2021;339:116598. doi: 10.1016/j.molliq.2021.116598.

33. Khaledian S, Kahrizi D, Balaky ST, Arkan E, Abdoli M, Martinez F. Electrospun nanofiber patch based on gum tragacanth/polyvinyl alcohol/molybdenum disulfide composite for tetracycline delivery and their inhibitory effect on Gram+ and Gram–bacteria. J Mol Liq 2021 Jul 15;334:115989. doi: 10.1016/j.molliq.2021.115989.

34. Khaledian S, Kahrizi D, Moradi S, Martinez F. An experimental and computational study to evaluation of chitosan/gum tragacanth coated-natural lipid-based nanocarriers for sunitinib delivery. J Mol Liq 2021 Jul 15;334:116075. doi: 10.1016/j.molliq.2021.116075.

35. Rafiee E, Kahrizi M. Collaboration of Ni, polyoxometalates and layered double hydroxides: synthesis, characterization, electrochemical and mechanism investigations as nano-catalyst in the Heck coupling reaction. Res Chem Intermed 2018;44(12):7289-309. doi: 10.1007/s11164-018-3557-z.

36. Olfati A, Kahrizi D, Balaky ST, Sharifi R, Tahir MB, Darvishi E. Green synthesis of nanoparticles using Calendula officinalis extract from silver sulfate and their antibacterial effects on Pectobacterium caratovorum. Inorg Chem Commun 2021;125:108439. doi: 10.1016/j.inoche.2020.108439.

37. Darvishi E, Kahrizi D, Arkan E. Comparison of different properties of zinc oxide nanoparticles synthesized by the green (using Juglans regia L. leaf extract) and chemical methods. J Mol Liq 2019;286:110831. doi: 10.1016/j.molliq.2019.04.108.

38. Sarkhosh S, Kahrizi D, Darvishi E, Tourang M, Haghighi-Mood S, Vahedi P, Ercisli S. Effect of Zinc Oxide Nanoparticles (ZnO-NPs) on Seed Germination Characteristics in Two Brassicaceae Family Species: Camelina sativa and Brassica napus L. J Nanomat 2022;2022. doi: 10.1155/2022/1892759.